arXiv:1309.5681v1 [nucl-ex] 23 Sep 2013

Energy Dependence of Moments of Net-proton Multiplicity Distributions at RHIC

L. Adamczyk,[1] J. K. Adkins,[23] G. Agakishiev,[21] M. M. Aggarwal,[35] Z. Ahammed,[54] I. Alekseev,[19] J. Alford,[22] C. D. Anson,[32] A. Aparin,[21] D. Arkhipkin,[4] E. C. Aschenauer,[4] G. S. Averichev,[21] J. Balewski,[27] A. Banerjee,[54] Z. Barnovska,[14] D. R. Beavis,[4] R. Bellwied,[50] A. Bhasin,[20] A. K. Bhati,[35] P. Bhattarai,[49] H. Bichsel,[56] J. Bielcik,[13] J. Bielcikova,[14] L. C. Bland,[4] I. G. Bordyuzhin,[19] W. Borowski,[46] J. Bouchet,[22] A. V. Brandin,[30] S. G. Brovko,[6] S. Bültmann,[33] I. Bunzarov,[21] T. P. Burton,[4] J. Butterworth,[41] H. Caines,[57] M. Calderón de la Barca Sánchez,[6] D. Cebra,[6] R. Cendejas,[36] M. C. Cervantes,[48] P. Chaloupka,[13] Z. Chang,[48] S. Chattopadhyay,[54] H. F. Chen,[43] J. H. Chen,[45] L. Chen,[9] J. Cheng,[51] M. Cherney,[12] A. Chikanian,[57] W. Christie,[4] J. Chwastowski,[11] M. J. M. Codrington,[49] R. Corliss,[27] J. G. Cramer,[56] H. J. Crawford,[5] X. Cui,[43] S. Das,[16] A. Davila Leyva,[49] L. C. De Silva,[50] R. R. Debbe,[4] T. G. Dedovich,[21] J. Deng,[44] A. A. Derevschikov,[37] R. Derradi de Souza,[8] S. Dhamija,[18] B. di Ruzza,[4] L. Didenko,[4] C. Dilks,[36] F. Ding,[6] P. Djawotho,[48] X. Dong,[26] J. L. Drachenberg,[53] J. E. Draper,[6] C. M. Du,[25] L. E. Dunkelberger,[7] J. C. Dunlop,[4] L. G. Efimov,[21] J. Engelage,[5] K. S. Engle,[52] G. Eppley,[41] L. Eun,[26] O. Evdokimov,[10] R. Fatemi,[23] S. Fazio,[4] J. Fedorisin,[21] P. Filip,[21] E. Finch,[57] Y. Fisyak,[4] C. E. Flores,[6] C. A. Gagliardi,[48] D. R. Gangadharan,[32] D. Garand,[38] F. Geurts,[41] A. Gibson,[53] M. Girard,[55] S. Gliske,[2] D. Grosnick,[53] Y. Guo,[43] A. Gupta,[20] S. Gupta,[20] W. Guryn,[4] B. Haag,[6] O. Hajkova,[13] A. Hamed,[48] L-X. Han,[45] R. Haque,[31] J. W. Harris,[57] J. P. Hays-Wehle,[27] S. Heppelmann,[36] A. Hirsch,[38] G. W. Hoffmann,[49] D. J. Hofman,[10] S. Horvat,[57] B. Huang,[4] H. Z. Huang,[7] P. Huck,[9] T. J. Humanic,[32] G. Igo,[7] W. W. Jacobs,[18] H. Jang,[24] E. G. Judd,[5] S. Kabana,[46] D. Kalinkin,[19] K. Kang,[51] K. Kauder,[10] H. W. Ke,[9] D. Keane,[22] A. Kechechyan,[21] A. Kesich,[6] Z. H. Khan,[10] D. P. Kikola,[38] I. Kisel,[15] A. Kisiel,[55] D. D. Koetke,[53] T. Kollegger,[15] J. Konzer,[38] I. Koralt,[33] W. Korsch,[23] L. Kotchenda,[30] P. Kravtsov,[30] K. Krueger,[2] I. Kulakov,[15] L. Kumar,[31] R. A. Kycia,[11] M. A. C. Lamont,[4] J. M. Landgraf,[4] K. D. Landry,[7] J. Lauret,[4] A. Lebedev,[4] R. Lednicky,[21] J. H. Lee,[4] W. Leight,[27] M. J. LeVine,[4] C. Li,[43] W. Li,[45] X. Li,[38] X. Li,[47] Y. Li,[51] Z. M. Li,[9] L. M. Lima,[42] M. A. Lisa,[32] F. Liu,[9] T. Ljubicic,[4] W. J. Llope,[41] R. S. Longacre,[4] X. Luo,[9] G. L. Ma,[45] Y. G. Ma,[45] D. M. M. D. Madagodagettige Don,[12] D. P. Mahapatra,[16] R. Majka,[57] S. Margetis,[22] C. Markert,[49] H. Masui,[26] H. S. Matis,[26] D. McDonald,[41] T. S. McShane,[12] N. G. Minaev,[37] S. Mioduszewski,[48] B. Mohanty,[31] M. M. Mondal,[48] D. A. Morozov,[37] M. G. Munhoz,[42] M. K. Mustafa,[38] B. K. Nandi,[17] Md. Nasim,[31] T. K. Nayak,[54] J. M. Nelson,[3] L. V. Nogach,[37] S. Y. Noh,[24] J. Novak,[29] S. B. Nurushev,[37] G. Odyniec,[26] A. Ogawa,[4] K. Oh,[39] A. Ohlson,[57] V. Okorokov,[30] E. W. Oldag,[49] R. A. N. Oliveira,[42] M. Pachr,[13] B. S. Page,[18] S. K. Pal,[54] Y. X. Pan,[7] Y. Pandit,[10] Y. Panebratsev,[21] T. Pawlak,[55] B. Pawlik,[34] H. Pei,[9] C. Perkins,[5] W. Peryt,[55] A. Peterson,[32] P. Pile,[4] M. Planinic,[58] J. Pluta,[55] D. Plyku,[33] N. Poljak,[58] J. Porter,[26] A. M. Poskanzer,[26] N. K. Pruthi,[35] M. Przybycien,[1] P. R. Pujahari,[17] H. Qiu,[26] A. Quintero,[22] S. Ramachandran,[23] R. Raniwala,[40] S. Raniwala,[40] R. L. Ray,[49] C. K. Riley,[57] H. G. Ritter,[26] J. B. Roberts,[41] O. V. Rogachevskiy,[21] J. L. Romero,[6] J. F. Ross,[12] A. Roy,[54] L. Ruan,[4] J. Rusnak,[14] N. R. Sahoo,[54] P. K. Sahu,[16] I. Sakrejda,[26] S. Salur,[26] A. Sandacz,[55] J. Sandweiss,[57] E. Sangaline,[6] A. Sarkar,[17] J. Schambach,[49] R. P. Scharenberg,[38] A. M. Schmah,[26] W. B. Schmidke,[4] N. Schmitz,[28] J. Seger,[12] P. Seyboth,[28] N. Shah,[7] E. Shahaliev,[21] P. V. Shanmuganathan,[22] M. Shao,[43] B. Sharma,[35] W. Q. Shen,[45] S. S. Shi,[26] Q. Y. Shou,[45] E. P. Sichtermann,[26] R. N. Singaraju,[54] M. J. Skoby,[18] D. Smirnov,[4] N. Smirnov,[57] D. Solanki,[40] P. Sorensen,[4] U. G. deSouza,[42] H. M. Spinka,[2] B. Srivastava,[38] T. D. S. Stanislaus,[53] J. R. Stevens,[27] R. Stock,[15] M. Strikhanov,[30] B. Stringfellow,[38] A. A. P. Suaide,[42] M. Sumbera,[14] X. Sun,[26] X. M. Sun,[26] Y. Sun,[43] Z. Sun,[25] B. Surrow,[47] D. N. Svirida,[19] T. J. M. Symons,[26] A. Szanto de Toledo,[42] J. Takahashi,[8] A. H. Tang,[4] Z. Tang,[43] T. Tarnowsky,[29] J. H. Thomas,[26] A. R. Timmins,[50] D. Tlusty,[14] M. Tokarev,[21] S. Trentalange,[7] R. E. Tribble,[48] P. Tribedy,[54] B. A. Trzeciak,[55] O. D. Tsai,[7] J. Turnau,[34] T. Ullrich,[4] D. G. Underwood,[2] G. Van Buren,[4] G. van Nieuwenhuizen,[27] J. A. Vanfossen, Jr.,[22] R. Varma,[17] G. M. S. Vasconcelos,[8] A. N. Vasiliev,[37] R. Vertesi,[14] F. Videbæk,[4] Y. P. Viyogi,[54] S. Vokal,[21] A. Vossen,[18] M. Wada,[49] M. Walker,[27] F. Wang,[38] G. Wang,[7] H. Wang,[4] J. S. Wang,[25] X. L. Wang,[43] Y. Wang,[51] Y. Wang,[10] G. Webb,[23] J. C. Webb,[4] G. D. Westfall,[29] H. Wieman,[26] S. W. Wissink,[18] R. Witt,[52] Y. F. Wu,[9] Z. Xiao,[51] W. Xie,[38] K. Xin,[41] H. Xu,[25] N. Xu,[26] Q. H. Xu,[44] Y. Xu,[43] Z. Xu,[4] W. Yan,[51] C. Yang,[43] Y. Yang,[25] Y. Yang,[9] Z. Ye,[10] P. Yepes,[41] L. Yi,[38] K. Yip,[4] I-K. Yoo,[39] Y. Zawisza,[43] H. Zbroszczyk,[55] W. Zha,[43] J. B. Zhang,[9] S. Zhang,[45] X. P. Zhang,[51] Y. Zhang,[43] Z. P. Zhang,[43] F. Zhao,[7] J. Zhao,[45] C. Zhong,[45] X. Zhu,[51] Y. H. Zhu,[45] Y. Zoulkarneeva,[21] and M. Zyzak[15]

(STAR Collaboration)

[1] *AGH University of Science and Technology, Cracow, Poland*
[2] *Argonne National Laboratory, Argonne, Illinois 60439, USA*

[3]University of Birmingham, Birmingham, United Kingdom
[4]Brookhaven National Laboratory, Upton, New York 11973, USA
[5]University of California, Berkeley, California 94720, USA
[6]University of California, Davis, California 95616, USA
[7]University of California, Los Angeles, California 90095, USA
[8]Universidade Estadual de Campinas, Sao Paulo, Brazil
[9]Central China Normal University (HZNU), Wuhan 430079, China
[10]University of Illinois at Chicago, Chicago, Illinois 60607, USA
[11]Cracow University of Technology, Cracow, Poland
[12]Creighton University, Omaha, Nebraska 68178, USA
[13]Czech Technical University in Prague, FNSPE, Prague, 115 19, Czech Republic
[14]Nuclear Physics Institute AS CR, 250 68 Řež/Prague, Czech Republic
[15]Frankfurt Institute for Advanced Studies FIAS, Germany
[16]Institute of Physics, Bhubaneswar 751005, India
[17]Indian Institute of Technology, Mumbai, India
[18]Indiana University, Bloomington, Indiana 47408, USA
[19]Alikhanov Institute for Theoretical and Experimental Physics, Moscow, Russia
[20]University of Jammu, Jammu 180001, India
[21]Joint Institute for Nuclear Research, Dubna, 141 980, Russia
[22]Kent State University, Kent, Ohio 44242, USA
[23]University of Kentucky, Lexington, Kentucky, 40506-0055, USA
[24]Korea Institute of Science and Technology Information, Daejeon, Korea
[25]Institute of Modern Physics, Lanzhou, China
[26]Lawrence Berkeley National Laboratory, Berkeley, California 94720, USA
[27]Massachusetts Institute of Technology, Cambridge, MA 02139-4307, USA
[28]Max-Planck-Institut für Physik, Munich, Germany
[29]Michigan State University, East Lansing, Michigan 48824, USA
[30]Moscow Engineering Physics Institute, Moscow Russia
[31]National Institute of Science Education and Research, Bhubaneswar 751005, India
[32]Ohio State University, Columbus, Ohio 43210, USA
[33]Old Dominion University, Norfolk, VA, 23529, USA
[34]Institute of Nuclear Physics PAN, Cracow, Poland
[35]Panjab University, Chandigarh 160014, India
[36]Pennsylvania State University, University Park, Pennsylvania 16802, USA
[37]Institute of High Energy Physics, Protvino, Russia
[38]Purdue University, West Lafayette, Indiana 47907, USA
[39]Pusan National University, Pusan, Republic of Korea
[40]University of Rajasthan, Jaipur 302004, India
[41]Rice University, Houston, Texas 77251, USA
[42]Universidade de Sao Paulo, Sao Paulo, Brazil
[43]University of Science & Technology of China, Hefei 230026, China
[44]Shandong University, Jinan, Shandong 250100, China
[45]Shanghai Institute of Applied Physics, Shanghai 201800, China
[46]SUBATECH, Nantes, France
[47]Temple University, Philadelphia, Pennsylvania, 19122, USA
[48]Texas A&M University, College Station, Texas 77843, USA
[49]University of Texas, Austin, Texas 78712, USA
[50]University of Houston, Houston, TX, 77204, USA
[51]Tsinghua University, Beijing 100084, China
[52]United States Naval Academy, Annapolis, MD 21402, USA
[53]Valparaiso University, Valparaiso, Indiana 46383, USA
[54]Variable Energy Cyclotron Centre, Kolkata 700064, India
[55]Warsaw University of Technology, Warsaw, Poland
[56]University of Washington, Seattle, Washington 98195, USA
[57]Yale University, New Haven, Connecticut 06520, USA
[58]University of Zagreb, Zagreb, HR-10002, Croatia

(Dated: February 26, 2022)

We report the beam energy ($\sqrt{s_{\rm NN}}$ = 7.7 - 200 GeV) and collision centrality dependence of the mean (M), standard deviation (σ), skewness (S), and kurtosis (κ) of the net-proton multiplicity distributions in Au+Au collisions. The measurements are carried out by the STAR experiment at midrapidity ($|y| < 0.5$) and within the transverse momentum range $0.4 < p_{\rm T} < 0.8$ GeV/c in the first phase of the Beam Energy Scan program at the Relativistic Heavy Ion Collider. These measurements are important for understanding the Quantum Chromodynamic (QCD) phase diagram.

The products of the moments, $S\sigma$ and $\kappa\sigma^2$, are sensitive to the correlation length of the hot and dense medium created in the collisions and are related to the ratios of baryon number susceptibilities of corresponding orders. The products of moments are found to have values significantly below the Skellam expectation and close to expectations based on independent proton and anti-proton production. The measurements are compared to a transport model calculation to understand the effect of acceptance and baryon number conservation, and also to a hadron resonance gas model.

PACS numbers: 25.75.Gz,12.38.Mh,21.65.Qr,25.75.-q,25.75.Nq

The Beam Energy Scan (BES) program at the Relativistic Heavy-Ion Collider (RHIC) facility aims at studying in detail the QCD phase structure. This enables us to map the phase diagram, temperature (T) versus baryonic chemical potential ($\mu_{\rm B}$), of strong interactions. Important advancements have been made towards the understanding of the QCD phase structure at small $\mu_{\rm B}$. Theoretically, it has been found that at high temperatures, there occurs a cross-over transition from hadronic matter to a de-confined state of quarks and gluons at $\mu_{\rm B} = 0$ MeV [1]. Experimental data from RHIC and the Large Hadron Collider have provided evidence of the formation of QCD matter with quark and gluon degrees of freedom [2]. Several studies have been done to estimate the quark-hadron transition temperature at $\mu_{\rm B} = 0$ [3]. Interesting features of the QCD phase structure are expected to appear at larger $\mu_{\rm B}$ [4]. These include the QCD critical point (CP) [5, 6] and a first order phase boundary between quark-gluon and hadronic phases [7].

Previous studies of net-proton multiplicity distributions suggest that the possible CP region is unlikely to be below $\mu_{\rm B} = 200$ MeV [8]. The versatility of the RHIC machine has permitted the center of mass energy ($\sqrt{s_{\rm NN}}$) to be varied below the injection energy ($\sqrt{s_{\rm NN}} = 19.6$ GeV), thereby providing the possibility to scan the QCD phase diagram above $\mu_{\rm B} \sim 250$ MeV. The $\mu_{\rm B}$ value is observed to increase with decreasing $\sqrt{s_{\rm NN}}$ [9]. The goal of the BES program at RHIC is to look for the experimental signatures of a first order phase transition and the critical point by colliding Au ions at various $\sqrt{s_{\rm NN}}$ [10].

Non-monotonic variations of observables related to the moments of the distributions of conserved quantities such as net-baryon, net-charge, and net-strangeness [11] number with $\sqrt{s_{\rm NN}}$ are believed to be good signatures of a phase transition and a CP. The moments are related to the correlation length (ξ) of the system [12]. The signatures of phase transition or CP are detectable if they survive the evolution of the system [13]. Finite size and time effects in heavy-ion collisions put constraints on the significance of the desired signals. A theoretical calculation suggests a non-equilibrium $\xi \approx$ 2-3 fm for heavy-ion collisions [14]. Hence, it is proposed to study the higher moments (like skewness, $S = \left\langle (\delta N)^3 \right\rangle / \sigma^3$ and kurtosis, $\kappa = \left[\left\langle (\delta N)^4 \right\rangle / \sigma^4 \right] - 3$ with $\delta N = N - \langle N \rangle$) of distributions of conserved quantities due to a stronger dependence on ξ [12]. Both the magnitude and the sign of the moments [15], which quantify the shape of the multiplicity distributions, are important for understanding phase transition and CP effects. Further, products of the moments can be related to susceptibilities associated with the conserved numbers. The product $\kappa\sigma^2$ of the net-baryon number distribution is related to the ratio of fourth order ($\chi_{\rm B}^{(4)}$) to second order ($\chi_{\rm B}^{(2)}$) baryon number susceptibilities [16, 17]. The ratio $\chi_{\rm B}^{(4)}/\chi_{\rm B}^{(2)}$ is expected to deviate from unity near the CP. It has different values for the hadronic and partonic phases [17].

This Letter reports measurements of the energy dependence of higher moments of the net-proton multiplicity ($N_p - N_{\bar{p}} = \Delta N_p$) distributions from Au+Au collisions. The aim is to search for signatures of the CP over a broad range of μ_B in the QCD phase diagram. Theoretical calculations have shown that ΔN_p fluctuations reflect the singularity of the charge and baryon number susceptibility, as expected at the CP [18]. The measurements presented here are within a finite acceptance range and only use the protons among the produced baryons. Refs. [19, 20] discuss the advantages of using net-baryon measurements and effects of acceptance on which the measurements depend intrinsically (e.g. conservation laws and other finite statistical fluctuations dominate near full and small acceptance respectively).

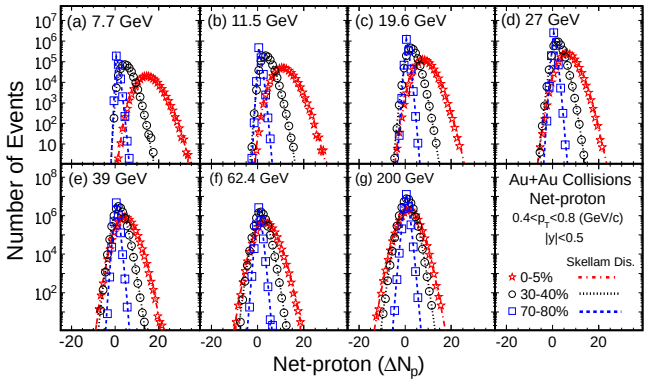


FIG. 1: (Color online) ΔN_p multiplicity distributions in Au+Au collisions at various $\sqrt{s_{\rm NN}}$ for 0-5%, 30-40% and 70-80% collision centralities at midrapidity. The statistical errors are small and within the symbol size. The lines are the corresponding Skellam distributions. The distributions are not corrected for the finite centrality width effect and $N_p(N_{\bar{p}})$ reconstruction efficiency.

The data presented in the paper were obtained using

the Time Projection Chamber (TPC) of the Solenoidal Tracker at RHIC (STAR) [21]. The event-by-event proton (N_p) and anti-proton ($N_{\bar{p}}$) multiplicities are measured for Au+Au minimum-bias events at $\sqrt{s_{\rm NN}}$ = 11.5, 19.6, 27, 39, 62.4, and 200 GeV for collisions occurring within ΔZ = 30 cm from the TPC center along the beam line. For 7.7 GeV, ΔZ is 50 cm. The 19.6 and 27 GeV data were collected in the year 2011 and the other energies were taken in 2010. Interactions of the beam with the beam pipe are rejected by choosing events with a radial vertex position in the transverse plane of less than 2 cm. The numbers of events analyzed are 3×10^6, 6.6×10^6, 15×10^6, 30×10^6, 86×10^6, 47×10^6, and 238×10^6 for $\sqrt{s_{\rm NN}}$ = 7.7, 11.5, 19.6, 27, 39, 62.4, and 200 GeV, respectively. Similar studies have also been carried out in p+p collisions with 0.6 $\times10^6$ and 7×10^6 events at $\sqrt{s_{\rm NN}}$ = 62.4 and 200 GeV, respectively. The centrality selection utilizes the uncorrected charged particle multiplicity other than identified protons and anti-protons within pseudorapidity $|\eta| < 1.0$ measured by the TPC. It is found that the measured net-proton moment values depend on the choice of the pseudorapidity range for the centrality selection. However the values of the moments do not change if the centrality selection range is further increased to the full acceptance of the TPC (which leads to a 15% increase in charged particle multiplicity). In the UrQMD [22] studies, after increasing the η range used for centrality selection to two units, it is observed that the maximum decrease of moments is $\sim$ 2.5% and 35% for $\sqrt{s_{\rm NN}}$ = 200 and 7.7 GeV, respectively [23]. There is minimal change for central collisions compared to other centralities. For each centrality, the average number of participants ($\langle N_{\rm part}\rangle$) is obtained by Glauber model calculations. The ΔN_p measurements are carried out at midrapidity ($|y| < 0.5$) in the range 0.4 $< p_{\rm T} <$ 0.8 GeV/c. Ionization energy loss (dE/dx) of charged particles in the TPC is used to identify the inclusive $p(\bar{p})$ [24]. The minimum $p_{\rm T}$ cut and a maximum distance of closest approach (DCA) to the collision vertex of 1 cm for each $p(\bar{p})$ candidate track suppress contamination from secondaries [24]. To have a good purity of the proton sample (better than 98%) for all beam energies, the maximum $p_{\rm T}$ is taken to be 0.8 GeV/c. This $p_{\rm T}$ interval accounts for approximately 50% of the total uncorrected $p + \bar{p}$ multiplicity at midrapidity. The average proton reconstruction efficiency for the $p_{\rm T}$ range studied is between 70-78% and 83-86%, for central and peripheral collisions, respectively, at different $\sqrt{s_{\rm NN}}$.

ΔN_p distributions from 70-80%, 30-40%, and 0-5% Au+Au collision centralities are shown in Fig. 1. The ΔN_p is not corrected for reconstruction efficiency. The distributions are also not corrected for the finite centrality width effect [23]. The subsequent analysis in this Letter is corrected for the centrality width effect. The corresponding Skellam distributions are also shown, $P(N) = \left(\frac{M_p}{M_{\bar{p}}}\right)^{N/2} I_N(2\sqrt{M_p M_{\bar{p}}}\,)\,\exp[-(M_p + M_{\bar{p}})]$, where $I_N(x)$ is a modified Bessel function of the first kind, and M_p and $M_{\bar{p}}$ are the measured mean multiplicities of proton and anti-protons [25]. The data seems to closely follow the Skellam distributions. To study the detail shape of the distribution, we discuss the various order cumulants (C_n), where $C_1 = M$, $C_2 = \sigma^2$, $C_3 = S\sigma^3$ and $C_4 = \kappa\sigma^4$. For both proton and anti-proton distributions being Poissonian, the $\Delta N_{\rm p}$ distribution will be a Skellam and have $C_3/C_2 = (M_p - M_{\bar{p}})/(M_p + M_{\bar{p}})$ and $C_4/C_2 = 1$.

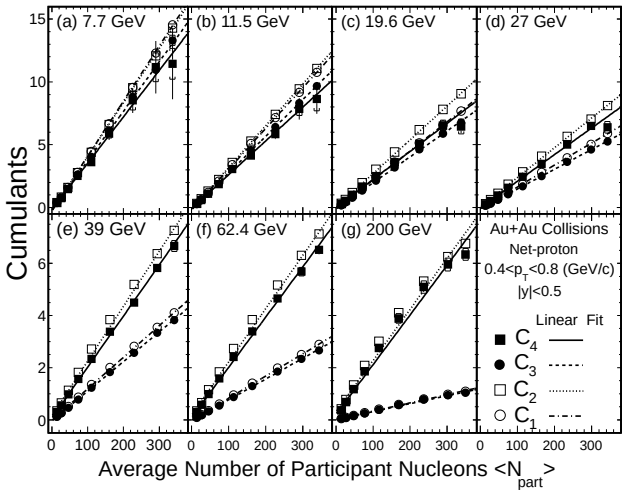


FIG. 2: Centrality dependence of the cumulants of ΔN_p distributions for Au+Au collisions. Error bars are statistical and caps are systematic errors.

The four cumulants that describe the shape of ΔN_p distributions at various collision energies are plotted as a function of $\langle N_{\rm part}\rangle$ in Fig. 2. We use the Delta theorem approach to obtain statistical errors [26]. The typical statistical error values for C_2, C_3, and C_4 for central Au+Au collisions at 7.7 GeV are 0.3%, 2.5% and 2.5% respectively, and those for high statistics 200 GeV results are 0.04%, 1.2% and 2.0% respectively. Most of the cumulant values show a linear variation with $\langle N_{\rm part}\rangle$. The C_1 values increase as $\sqrt{s_{\rm NN}}$ decreases, in accordance with the energy and centrality dependence of baryon transport. C_2 and C_4 have similar values as a function of $\langle N_{\rm part}\rangle$ for a given $\sqrt{s_{\rm NN}}$. C_1 and C_3 follow each other closely as a function of $\langle N_{\rm part}\rangle$ at any given $\sqrt{s_{\rm NN}}$. The differences between these groupings decrease as $\sqrt{s_{\rm NN}}$ decreases. The decrease in the C_3 values with increasing beam energy indicates that the distributions become symmetric for the higher beam energies. The particle production at any given centrality can be considered a superposition of several identically distributed independent sources the number of which is proportional to $N_{\rm part}$ [8]. For the cumulants, this means a linear increase with $\langle N_{\rm part}\rangle$ as the system volume increases. This reflects that the cu-

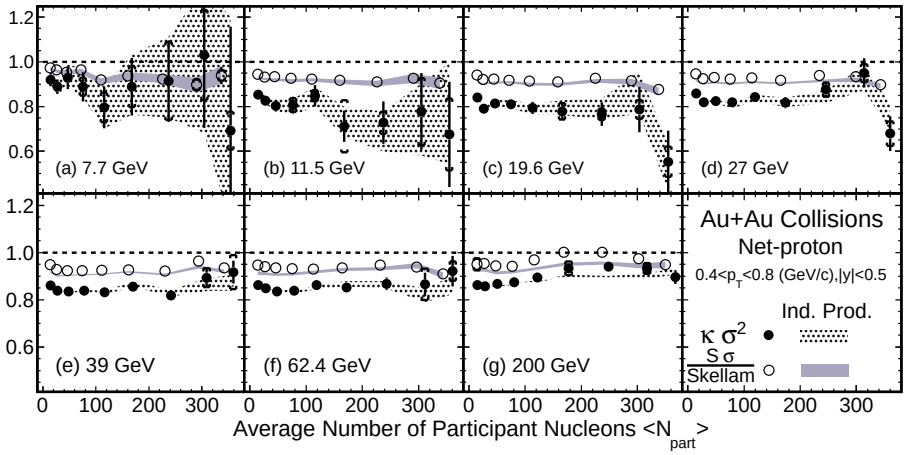


FIG. 3: (Color online) Centrality dependence of $S\sigma$/Skellam and $\kappa\sigma^2$ for ΔN_p in Au+Au collisions at $\sqrt{s_{\rm NN}}$ = 7.7, 11.5, 19.6, 27, 39, 62.4, and 200 GeV. The results are corrected for the $p(\bar{p})$ reconstruction efficiency. The error bars are statistical and caps are systematic errors. The shaded bands are expectations assuming the approach of independent proton and anti-proton production, as described in the text. The width of the bands represents statistical uncertainty.

mulants are extensive quantities that are proportional to system volume. The lines in Fig. 2 are linear fits to the cumulants, which provide a reasonable description of the centrality dependence. This indicates that the volume effect dominates the measured cumulants values. The χ^2/ndf between the linear fit and data are smaller than 3.2 for all cumulants presented. The slight deviation of some cumulants in most central collisions from the fit line are due to the corresponding proton distributions.

In order to cancel the volume effect to first order and to understand the collision dynamics, we present the ratios of the cumulants C_3/C_2 ($= S\sigma$) and C_4/C_2 ($= \kappa\sigma^2$) as a function of $\langle N_{\rm part}\rangle$ for all collision energies, in Fig. 3. The $S\sigma$ are normalized to the corresponding Skellam expectations. Results with correction for the $p(\bar{p})$ reconstruction efficiency are presented. The correction for a finite track reconstruction efficiency is done by assuming a binomial distribution for the probability to reconstruct n particles out of N produced [20, 27]. These observables are related to the ratio of baryon number susceptibilities ($\chi_{\rm B}$) at a given temperature (T) computed in QCD motivated models as: $S\sigma = (\chi_{\rm B}^{(3)}/T)/(\chi_{\rm B}^{(2)}/T^2)$ and $\kappa\sigma^2 = (\chi_{\rm B}^{(4)})/(\chi_{\rm B}^{(2)}/T^2)$ [16, 17]. Close to the CP, QCD based calculations predict the net-baryon number distributions to be non-Gaussian and susceptibilities to diverge, causing $S\sigma$ and $\kappa\sigma^2$ to have non-monotonic variations with $\langle N_{\rm part}\rangle$ and/or $\sqrt{s_{\rm NN}}$ [6, 12].

We observe in Fig. 3 the $\kappa\sigma^2$ and the $S\sigma$ normalized to Skellam expectations are below unity for all of the Au+Au collision data sets presented. The deviations below unity of the order of 1-3% [28] as seen for the central collisions for energies above 27 GeV are expected from quantum statistical effects. The measured $S\sigma$ and $\kappa\sigma^2$ are compared to expectations in which the cumulants of ΔN_p distributions are constructed by considering independent production of protons and anti-protons. For independent production, the various order (n = 1, 2, 3 and 4) net-proton cumulants are given as $C_n(\Delta N_p) = C_n(N_p) + (-1)^n C_n(N_{\bar{p}})$, where $C_n(N_p)$ and $C_n(N_{\bar{p}})$ are cumulants of the measured distributions of $N_{\rm p}$ and $N_{\bar{p}}$, respectively. This approach breaks intra-event correlations between N_p and $N_{\bar{p}}$. The results from independent production are found to be in good agreement with the data. However, for $\sqrt{s_{\rm NN}} < 39$ GeV, the C_n of net-protons are dominated by the corresponding values from the proton distributions. The assumption that N_p and $N_{\bar{p}}$ have independent binomial distributions [29] also leads to a good description of the measurements (similar to independent production, but not plotted in Fig. 3).

Systematic errors are estimated by varying the following requirements for $p(\bar{p})$ tracks: DCA, track quality reflected by the number of fit points used in track reconstruction, and the dE/dx selection criteria for $p(\bar{p})$ identification. The typical systematic errors are of the order 4% for M and σ, 5% for S and 12% for κ. A 5% uncertainty in reconstruction efficiency estimation is also considered. The statistical and systematic (caps) errors are presented separately in the figures.

Figure 4 shows the energy dependence of $S\sigma$ and $\kappa\sigma^2$ for ΔN_p for Au+Au collisions for two collision centralities (0-5% and 70-80%), corrected for $p(\bar{p})$ reconstruction efficiency. The $S\sigma$ values normalized to the corresponding Skellam expectations are shown in the bottom panel of Fig. 4. The Skellam expectations reflect a system of totally uncorrelated, statistically random particle production. The corresponding results from the p+p collisions are also shown and found to be similar to peripheral Au+Au collisions for $\sqrt{s_{\rm NN}}$ = 62.4 and 200 GeV within the statistical errors. For $\sqrt{s_{\rm NN}}$ below 39 GeV, differences are observed between the 0-5% central

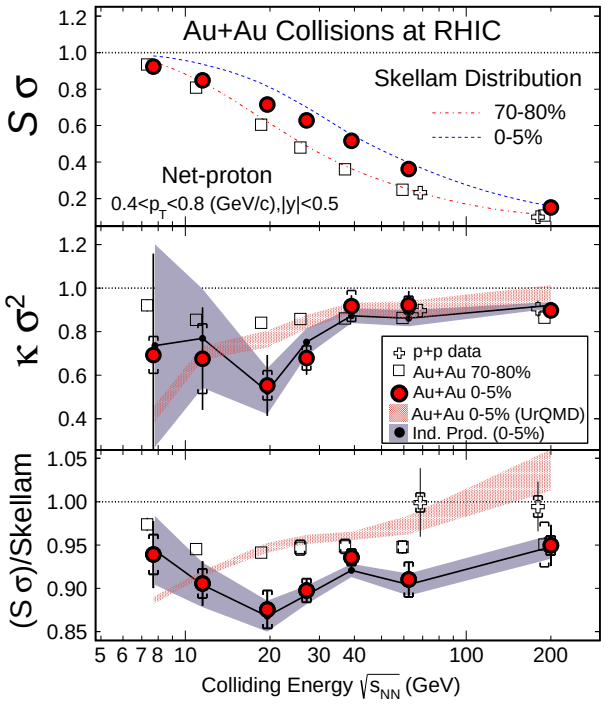


FIG. 4: (Color online) Collision energy and centrality dependence of the net-proton $S\sigma$ and $\kappa\sigma^2$ from Au+Au and p+p collisions at RHIC. Crosses, open squares and filled circles are for the efficiency corrected results of p+p, 70-80%, and 0-5% Au+Au collisions, respectively. Skellam distributions for corresponding collision centralities are shown in the top panel. Shaded hatched bands are the results from UrQMD [22]. In the middle and lower panels, the shaded solid bands are the expectations assuming independent proton and anti-proton production. The width of the bands represents statistical uncertainties. The hadron resonance gas model (HRG) values for $\kappa\sigma^2$ and $S\sigma$/Skellam are unity. The error bars are statistical and caps are systematic errors. For clarity, p+p and 70-80% Au+Au results are slightly displaced horizontally.

Au+Au collisions and the peripheral collisions. The results are closer to unity for $\sqrt{s_{\rm NN}}$ = 7.7 GeV. Deviations of 0-5% Au+Au data from Skellam expectations, $((|\,\text{Data}-\text{Skellam}\,|)/\sqrt{\text{err}_{\rm stat}{}^2+\text{err}_{\rm sys}{}^2})$ are found to be most significant for 19.6 GeV and 27 GeV, with values of 3.2 and 3.4 for $\kappa\sigma^2$, and 4.5 and 5.6 for $S\sigma$, respectively. The deviations for 5-10% Au+Au data are smaller for $\kappa\sigma^2$ with values of 2.0 and 0.6 and are 5.0 and 5.4 for $S\sigma$, for 19.6 GeV and 27 GeV, respectively. A reasonable description of the measurements is obtained from the independent production approach. The data also show deviations from the hadron resonance gas model [31, 32] which predict $\kappa\sigma^2$ and $S\sigma$/Skellam to be unity. To understand the effects of baryon number conservation [33] and experimental acceptance, UrQMD model calculations (a transport model which does not include a CP) [22] for 0-5% Au+Au collisions are shown in the middle and bottom panels of Fig. 4. The UrQMD model shows a monotonic decrease with decreasing beam energy [23].

The current data provide the most relevant measurements over the widest range in μ_B (20 to 450 MeV) to date for the CP search, and for comparison with the baryon number susceptibilities computed from QCD to understand the various features of the QCD phase structure [6, 16, 17]. The deviations of $S\sigma$ and $\kappa\sigma^2$ below Skellam expectation are qualitatively consistent with a QCD based model which includes a CP [34]. However the UrQMD model which does not include a CP also shows deviations from the Skellam expectation. Hence conclusions on the existence of CP can be made only after comparison to QCD calculations with CP behavior which include the dynamics associated with heavy-ion collisions, such as finite correlation length and freeze-out effects.

In summary, measurements of the higher moments and their products ($S\sigma$ and $\kappa\sigma^2$) of the net-proton distributions at midrapidity ($|y|<0.5$) within $0.4 < p_{\rm T} < 0.8$ GeV/c in Au+Au collisions over a wide range of $\sqrt{s_{\rm NN}}$ and $\mu_{\rm B}$ have been presented to search for a possible CP and signals of a phase transition in the collisions. These observables show a centrality and energy dependence, which are neither reproduced by non-CP transport model calculations, nor by a hadron resonance gas model. For $\sqrt{s_{\rm NN}} > 39$ GeV, $S\sigma$ and $\kappa\sigma^2$ values are similar for central, peripheral Au+Au collisions and p+p collisions. Deviations for both $\kappa\sigma^2$ and $S\sigma$ from HRG and Skellam expectations are observed for $\sqrt{s_{\rm NN}} \leq 27$ GeV. The measurements are reasonably described by assuming independent production of N_p and $N_{\bar{p}}$, indicating that there are no apparent correlations between the protons and anti-protons for the observable presented. However at the lower beam energies, the net-proton measurements are dominated by the shape of the proton distributions only. The data presented here also provides information to extract freeze-out conditions in heavy-ion collisions using QCD based approaches [35, 36].

We thank M. Asakawa, R. Gavai, S. Gupta, F. Karsch, K. Rajagopal, K. Redlich and M. A. Stephanov for discussions related to this work. We thank the RHIC Operations Group and RCF at BNL, and the NERSC Center at LBNL, the KISTI Center in Korea and the Open Science Grid consortium for providing resources and support. This work was supported in part by the Offices of NP and HEP within the U.S. DOE Office of Science, the U.S. NSF, CNRS/IN2P3, FAPESP CNPq of Brazil, Ministry of Ed. and Sci. of the Russian Federation, NNSFC, CAS, MoST, and MoE of China, the Korean Research Foundation, GA and MSMT of the Czech Republic, FIAS of Germany, DAE, DST, and CSIR of the Government of India, National Science Centre of Poland, National Research Foundation (NRF-2012004024), Ministry of Sci., Ed. and Sports of the Rep. of Croatia, and RosAtom of Russia. Finally, we gratefully acknowledge a sponsored research grant for the 2006 run period from Renaissance Technologies Corporation.

[1] Y. Aoki *et al.*, Nature **443**, 675 (2006).

[2] I. Arsene *et al.*, Nucl. Phys. A **757**, 1 (2005); B. B. Back *et al.*, Nucl. Phys. A **757**, 28 (2005); J. Adams *et al.*, Nucl. Phys. A **757**, 102 (2005); K. Adcox *et al.*, Nucl. Phys. A **757**, 184 (2005); S. Chatrchyan *et al.*, JHEP **05**, 063 (2012); B. Abelev *et al.*, Phys. Rev. Lett. **109**, 072301 (2012).

[3] Y. Aoki *et al.*, Phys. Lett. B **643**, 46 (2006); M. Cheng *et al.*, Phys. Rev. D **74**, 054507 (2006).

[4] K. Fukushima and T. Hatsuda, Rept. Prog. Phys. **74**, 014001 (2011).

[5] M. A. Stephanov, Prog. Theor. Phys. Suppl. **153**, 139 (2004) [Int. J. Mod. Phys. A **20**, 4387 (2005)]; Z. Fodor and S. D. Katz, JHEP **04**, 050 (2004).

[6] R. V. Gavai and S. Gupta, Phys. Rev. D **78**, 114503 (2008); Phys. Rev. D **71**, 114014 (2005); S. Gupta, PoS CPOD **2009**, 025 (2009).

[7] S. Ejiri, Phys. Rev. D **78**, 074507 (2008); E. S. Bowman and J. I. Kapusta, Phys. Rev. C **79**, 015202 (2009).

[8] M. M. Aggarwal *et al.*, Phys. Rev. Lett. **105**, 022302 (2010).

[9] J. Cleymans *et al.*, Phys. Rev. C **73**, 034905 (2006).

[10] B. I. Abelev *et al.*, Phys. Rev. **C 81**, 024911 (2010); STAR Internal Note - SN0493, 2009.

[11] V. Koch, A. Majumder and J. Randrup, Phys. Rev. Lett. **95**, 182301 (2005); M. Asakawa, U. W. Heinz and B. Muller, Phys. Rev. Lett. **85**, 2072 (2000).

[12] M. A. Stephanov, Phys. Rev. Lett. **102**, 032301 (2009); C. Athanasiou *et al.*, Phys. Rev. D **82**, 074008 (2010).

[13] M. A. Stephanov, Phys. Rev. D **81**, 054012 (2010).

[14] B. Berdnikov and K. Rajagopal, Phys. Rev. D **61**, 105017 (2000).

[15] M. Asakawa, S. Ejiri and M. Kitazawa, Phys. Rev. Lett. **103**, 262301 (2009); M. A. Stephanov, Phys. Rev. Lett. **107**, 052301 (2011).

[16] S. Ejiri, F. Karsch and K. Redlich, Phys. Lett. B **633**, 275 (2006); M. Cheng *et al.*, Phys. Rev. **D 79**, 074505 (2009); B. Stokic *et al.*, Phys. Lett. **B 673**, 192 (2009); S. Gupta *et al.*, Science **332**, 1525 (2011).

[17] R. V. Gavai and S. Gupta, Phys. Lett. B **696**, 459 (2011).

[18] Y. Hatta and M. A. Stephanov, Phys. Rev. Lett. **91**, 102003 (2003).

[19] M. Kitazawa and M. Asakawa, Phys. Rev. C **86**, 024904 (2012) [Erratum-ibid. C **86**, 069902 (2012)].

[20] A. Bzdak and V. Koch, Phys. Rev. C **86**, 044904 (2012).

[21] K. H. Ackermann *et al.*, Nucl. Instr. Meth. **A 499**, 624 (2003).

[22] M. Bleicher *et al.*, J. Phys. G **25**, 1859 (1999).

[23] X. Luo, J. Xu, B. Mohanty and N. Xu, J. Phys. G **40**, 105104 (2013).

[24] B. I. Abelev *et al.*, Phys. Rev. **C 79**, 034909 (2009); Phys. Lett. **B 655**, 104 (2007).

[25] P. Braun-Munzinger *et al.*, Phys. Rev. C **84**, 064911 (2011).

[26] X. Luo, J. Phys. G **39**, 025008 (2012).

[27] $C_2^{X-Y} = (C_2^{x-y} + (\varepsilon-1)(\langle x\rangle + \langle y\rangle))/\varepsilon^2$; $C_3^{X-Y} = (C_3^{x-y} + 3(\varepsilon-1)(C_2^x - C_2^y) + (\varepsilon-1)(\varepsilon-2)(\langle x\rangle - \langle y\rangle))/\varepsilon^3$ and $C_4(X-Y) = (C_4(x-y) - 2(\varepsilon-1)C_3(x+y) + 8(\varepsilon-1)(C_3(x)+C_3(y)) + (5-\varepsilon)(\varepsilon-1)C_2(x+y) + 8(\varepsilon-2)(\varepsilon-1)(C_2(x)+C_2(y)) + (\varepsilon^2-6\varepsilon+6)(\varepsilon-1)(\langle x\rangle + \langle y\rangle))/\varepsilon^4$. Where (X,Y) and (x,y) are the numbers of $(p,\bar{p})$ produced and measured respectively. ε is the $p(\bar{p})$ reconstruction efficiency.

[28] M. A. Stephanov, K. Rajagopal and E. V. Shuryak, Phys. Rev. D **60**, 114028 (1999).

[29] T. J. Tarnowsky and G. D. Westfall, Phys. Lett. B **724**, 51 (2013).

[30] M. Gyulassy and X.-N. Wang, Comput. Phys. Commun. **83**, 307 (1994).

[31] F. Karsch and K. Redlich, Phys. Lett. B **695**, 136 (2011).

[32] P. Garg *et al.*, arXiv:1304.7133 [nucl-ex].

[33] A. Bzdak, V. Koch and V. Skokov, Phys. Rev. C **87**, 014901 (2013).

[34] M. A. Stephanov, J. Phys. G **38**, 124147 (2011).

[35] A. Bazavov *et al.*, Phys. Rev. Lett. **109**, 192302 (2012).

[36] S. Borsanyi *et al.*, arXiv:1305.5161 [hep-lat].